Annals of Diagnostic Pathology 47 (2020) 151518

Contents lists available at ScienceDirect

Annals of Diagnostic Pathology

journal homepage: www.elsevier.com/locate/anndiagpath

Original Contribution

Automated quantification and architectural pattern detection of hepatic fibrosis in NAFLD

Samer Gawrieh[a,*], Deepak Sethunath[b], Oscar W. Cummings[c], David E. Kleiner[d], Raj Vuppalanchi[a], Naga Chalasani[a], Mihran Tuceryan[b]

[a] Division of Gastroenterology and Hepatology, Indiana University School of Medicine, Indianapolis, IN, United States of America
[b] Department of Computer and Information Science, Indiana University Purdue University, Indianapolis, IN, United States of America
[c] Department of Pathology and Laboratory Medicine, Indiana University School of Medicine, Indianapolis, IN, United States of America
[d] Laboratory of Pathology, National Cancer Institute, Bethesda, MD, United States of America

ARTICLE INFO

Keywords:
NASH
Artificial intelligence
Automation
Digital image analysis

ABSTRACT

Accurate detection and quantification of hepatic fibrosis remain essential for assessing the severity of non-alcoholic fatty liver disease (NAFLD) and its response to therapy in clinical practice and research studies. Our aim was to develop an integrated artificial intelligence-based automated tool to detect and quantify hepatic fibrosis and assess its architectural pattern in NAFLD liver biopsies. Digital images of the trichrome-stained slides of liver biopsies from patients with NAFLD and different severity of fibrosis were used. Two expert liver pathologists semi-quantitatively assessed the severity of fibrosis in these biopsies and using a web applet provided a total of 987 annotations of different fibrosis types for developing, training and testing supervised machine learning models to detect fibrosis. The collagen proportionate area (CPA) was measured and correlated with each of the pathologists semi-quantitative fibrosis scores. Models were created and tested to detect each of six potential fibrosis patterns. There was good to excellent correlation between CPA and the pathologist score of fibrosis stage. The coefficient of determination (R^2) of automated CPA with the pathologist stages ranged from 0.60 to 0.86. There was considerable overlap in the calculated CPA across different fibrosis stages. For identification of fibrosis patterns, the models areas under the receiver operator curve were 78.6% for detection of periportal fibrosis, 83.3% for pericellular fibrosis, 86.4% for portal fibrosis and > 90% for detection of normal fibrosis, bridging fibrosis, and presence of nodule/cirrhosis. In conclusion, an integrated automated tool could accurately quantify hepatic fibrosis and determine its architectural patterns in NAFLD liver biopsies.

1. Introduction

Hepatic fibrosis is a complex and dynamic wound healing response to chronic liver injury resulting from any chronic liver disease [1]. Progression of liver disease is marked by increased accumulation of hepatic fibrosis which leads to hepatic architectural changes, development of cirrhosis, portal hypertension and ultimately liver failure [2]. In addition to its important role in monitoring disease progression and guiding treatment decisions, accurate detection and quantification of hepatic fibrosis remain essential for assessing the severity of liver disease and response to therapy in clinical practice, research studies, and clinical trials.

Traditionally, assessment of hepatic fibrosis has relied on semi-quantitative histological evaluation systems of liver biopsy samples [3-6]. The remarkable progress in developing non-invasive methods to detect and quantify hepatic fibrosis has not eliminated the need for liver biopsy, which remains the gold standard for assessing liver histology and fibrosis both in practice and research [7,8]. Ranging from 0 to 6 [3-6], the numbers assigned to the fibrosis stage in different semi-quantitative systems reflect increasing severity of liver disease based on quantity, location and architectural pattern of fibrosis. Although manual semi-quantitative systems are very useful tools for measuring fibrosis, interest in more reproducible, continuous and precise methods in detecting changes in fibrosis triggered the search for automated methods based on digital image analysis (DIA) of liver biopsies [9-14].

Over the past two decades, many studies based on DIA used different computer-assisted automated algorithms to provide continuous quantification of fibrosis in liver biopsy images, typically by providing

* Corresponding author at: Division of Gastroenterology and Hepatology, Indiana University School of Medicine, 702 Rotary Circle, Suite 225, Indianapolis, IN 46202, United States of America.
E-mail address: sgawrieh@iu.edu (S. Gawrieh).

https://doi.org/10.1016/j.anndiagpath.2020.151518

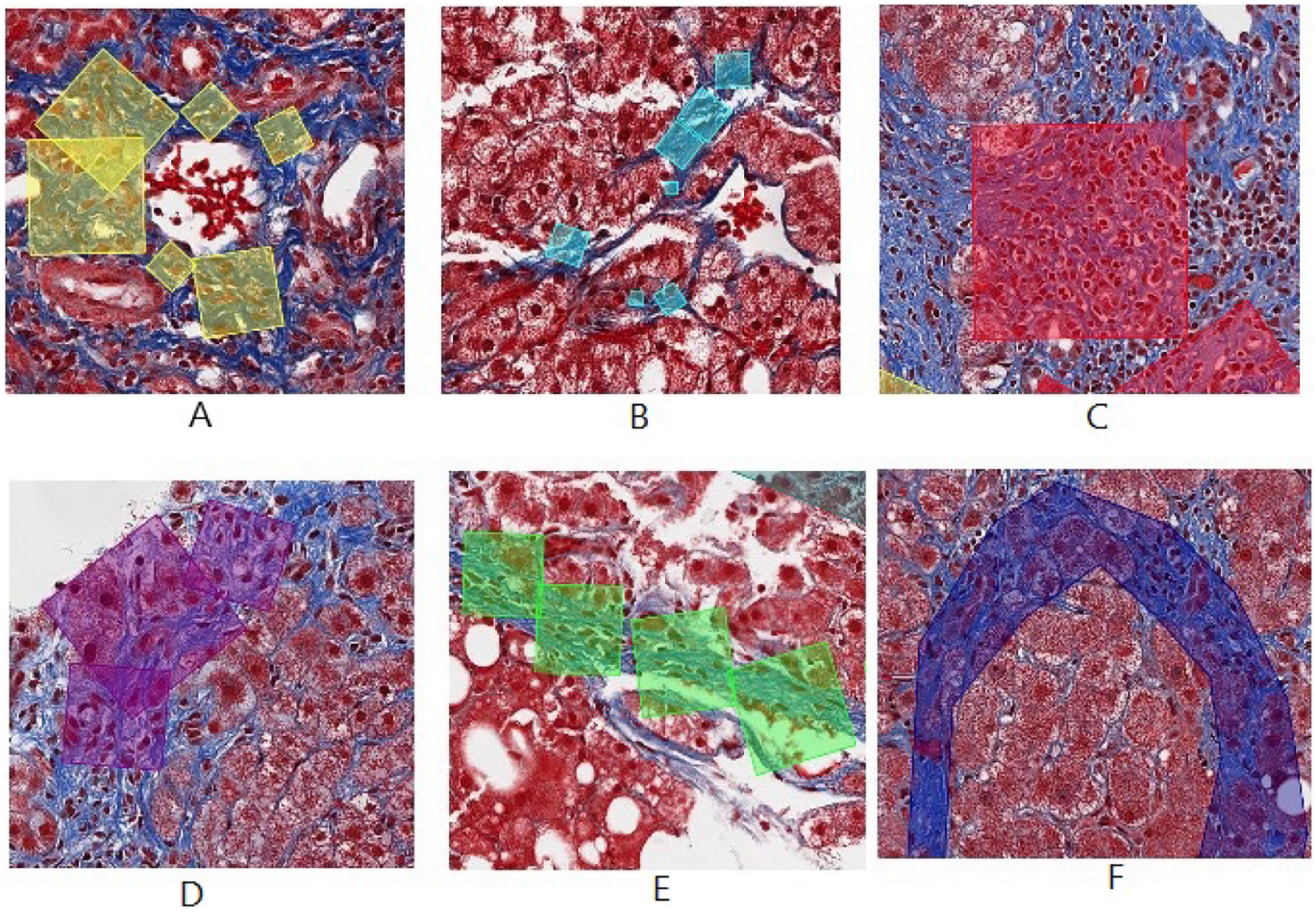

Fig. 1. Different types of fibrosis annotated. A. Normal Fibrosis B. Pericellular Fibrosis C. Portal Fibrosis D. Periportal Fibrosis E. Bridging Fibrosis F. Nodule.

the ratio of fibrotic area relative to the total liver tissue area [collagen proportionate area (CPA)] [9,15-18]. These studies demonstrated that automated measurement of fibrosis is highly correlated with semi-quantitative fibrosis stages [14,16-21], reproducible [9,15,22,23], and more sensitive than semi-quantitative histological staging in detecting changes in hepatic fibrosis [11,15,23]. Furthermore, CPA showed better correlation than semi-quantitative scores with measures of liver function [11,24], liver stiffness measured by transient elastography [21,25,26], and clinically significant portal hypertension [16,24,25,27]. In patients with cirrhosis, CPA was a stronger predictor of hepatic decompensation, hepatocellular carcinoma and liver-related death than semi-quantitative assessment of fibrosis [28-31].

However, these methods are not without problems; the amount of fibrosis measured by DIA may not reflect the architectural pattern or type of fibrosis distribution and there is a significant overlap in CPA across different semi-quantitative fibrosis stages [10,11,14,32]. The vast majority of these studies were conducted in patients with viral hepatitis C or B and some included additional liver diseases [20,27,33,34]. Only two prior studies attempted to detect location and patterns of fibrosis; one study in the setting of hepatitis C [9] and the other did not specify the liver disease studied [22]. There is however very little work done to automatically detect and quantify hepatic fibrosis or assess fibrosis architectural patterns in the setting of non-alcoholic fatty liver disease (NAFLD) [35,36].

NAFLD is now a leading cause of liver disease worldwide [37]. The presence of fibrosis and especially advanced fibrosis is a strong predictor of liver related outcomes in patients with NAFLD [38-40]. The fibrosis in NAFLD has a unique pattern that starts usually with accumulation of fibrosis around the central veins (perisinusoidal or pericellular pattern) [41]. Further, accurate quantification of fibrosis is important as improvement, stability, or worsening of fibrosis are important end points in the ever increasing number of therapeutic clinical trials for NAFLD and its severe phenotype, non-alcoholic steatohepatitis (NASH) [42,43].

In this study, we used artificial intelligence (AI) methods to develop an integrated automated tool to detect and quantify hepatic fibrosis and then assess its architectural pattern in NAFLD and NASH liver biopsies. We assess the correlation of the calculated CPA with expert pathologist semi-quantitative scores of fibrosis and internally validate the performance of the classifier.

2. Methods

This research protocol was reviewed and approved by the Internal Review Board of Indiana University School of Medicine. A set of digital images of the trichrome (TC) stained slides of 18 unique liver biopsy was used for this study. These biopsies covered the entire spectrum and severity of NAFLD and stages of fibrosis. The two study pathologists assessed fibrosis stage according to the NASH Clinical Research Network system [6].

The detailed methods used are provided in the supplementary material. Briefly, the biopsy slides were scanned at 20× using Aperio ScanScope CS system by Leica Biosystems (Buffalo Grove, IL) to obtain digitized images. Two expert liver pathologists used a web-based annotation tool we had built to provide annotations to train machine learning algorithms using the biopsy image data [44,45]. Fig. 1 shows an example annotation of liver fibrosis regions and types in a human liver biopsy image. All experiments conducted in this study to build

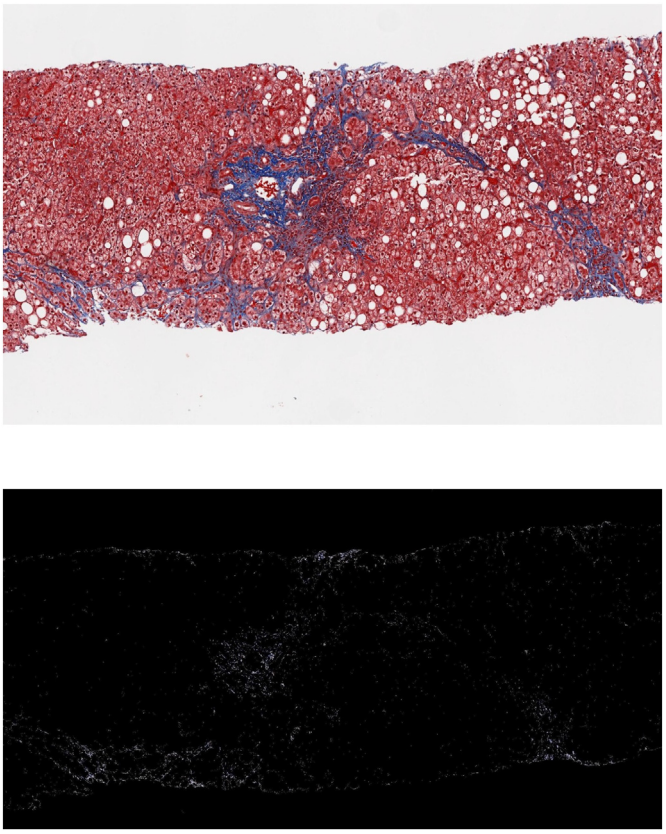

Fig. 2. An example of blue region detection in a trichrome stained sub-slide. A) A trichrome stained sub-slide. B) Blue regions detected in the trichrome stained sub-slide. (For interpretation of the references to color in this figure legend, the reader is referred to the web version of this article.)

different decision support systems to detect various histological features in a liver biopsy use the pathologists' annotations for building machine learning models and as well as the pathologists' semi-quantitative grades for correlation.

2.1. Quantification of fibrosis in liver biopsies

Collagen accounts for the majority of blue region present in a liver biopsy slide. Following image retrieval, liver tissue is identified from surrounding image background, and then a tissue mask is applied to identify blue regions (Fig. 2). Once the blue region extraction is done, the total quantity of the collagen is calculated as the sum of detected blue pixels in the image weighted by the amount of blue content in each pixel (i.e., the weight is the pixel value of the blue channel). The collagen proportionate area (CPA) is measured by calculating the percent of the blue region area to the total tissue area. This calculated CPA was then compared to the semi-quantitative grades assigned by the experts to the slide. The pathologists' fibrosis scores stage 1A, 1B, and 1C were treated as stage 1 for the correlation analysis [6].

2.2. Identification of fibrosis patterns

The flowchart of the approach of detecting collagen in the biopsy images and to identify different types of fibrosis is shown in Fig. 3. Briefly, this process involves the extraction of blue regions (collagen) in a TC stained liver biopsy and using different AI methods including supervised machine learning models and image segmentation techniques using features such as histogram of oriented gradients, speeded up robust features, and Gabor features. Fibrosis architectural patterns include normal, pericellular (perisinusoidal), portal, periportal, bridging, and nodule (cirrhosis) (Fig. 1). In order to detect the various types of fibrosis, supervised machine learning models were trained to detect each type separately, involving the extraction of blue regions in an image and performing various feature extraction techniques on the regions annotated by experts, which help uniquely identify the type of fibrosis content. As pathologist DEK provided large number of annotations for each type of fibrosis (Supplementary Table 1), his annotations were used for training the fibrosis classifiers. A supervised machine learning model using support vector machines (SVM) with linear kernel is used to build classifier models based on morphological structures, textural properties and their surrounding neighborhood of different types of fibrosis. For each of the blue regions extracted by using the steps above, different types of features are calculated. The blue regions, and their surrounding area of 20 pixels in all directions are also computed. After the classifier models for various types of fibrosis are built, the classifiers are verified by 10-fold cross-validation is done by holding 1/10th of the training samples, training the classifier using the 90% of the data and testing on the held out 1/10th of the labeled data and repeating it 10 times with different subsets. The statistics over the 10-fold repetition are then averaged (e.g., accuracy) in order to summarize performance.

The area under the receiver-operating curve (AUROC) is computed using the method implemented in WEKA tool (https://waikato.github.io/weka-wiki/auc/). WEKA tool implements this by generating points on the ROC curve as True positive rate also known as Recall (Y axis) vs. False positive rate (X axis). It then computes the area under this curve.

3. Results

3.1. Pathologists assessment of fibrosis

As shown in Fig. 4, the liver biopsies samples studied covered all severities of fibrosis in NAFLD and ranged from absence of fibrosis (stage 0) to cirrhosis (stage 4).

There was an overall excellent agreement between the two study pathologists on whether fibrosis was present (94.4%) and on the stage of fibrosis (complete agreement on the stage in 72.2% of biopsies, a difference in staging by 1 stage in 22.2%, and by 3 stages in only 5.5%).

A total of 987 annotations (normal fibrosis 186, pericellular fibrosis 254, portal fibrosis 120, periportal fibrosis 173, bridging fibrosis 139, nodule 115) were provided by the two study pathologists.

3.2. Correlation of collagen proportionate area with pathologists' fibrosis stage

There was good to excellent correlation between CPA and the pathologist score of fibrosis stage (Fig. 5). The coefficient of determination (R^2) of automated CPA with Pathologist DEK's stages is 0.607 and with Pathologist OWC's grades is 0.867.

As shown in Fig. 5, there was considerable overlap in the calculated CPA across different pathologist assigned fibrosis stages. For example, a CPA of 0.14 may be seen with fibrosis stages of 1–4 with pathologist DEK staging (Fig. 5A), whereas a CPA of 0.16 may be seen with fibrosis stages 2–4 with pathologist OWC (Fig. 5B).

Because CPA relies on color extraction methods where fibrosis is in shades of blue whereas steatosis is white, there was no technical difficulty in calculating the CPA regardless the steatosis severity. As expected, there was weak correlation between CPA and steatosis grade ($R^2 < 0.2$), and at any given steatosis grade, different severities of CPA were calculated (Supplementary Fig. 1).

3.3. Identification of fibrosis architectural subtypes

As shown in Table 1, the models performance was fair for detection of periportal fibrosis (AUROC 78.6%), good for detecting pericellular and portal fibrosis (AUROC 83.3% and 86.4%, respectively), and

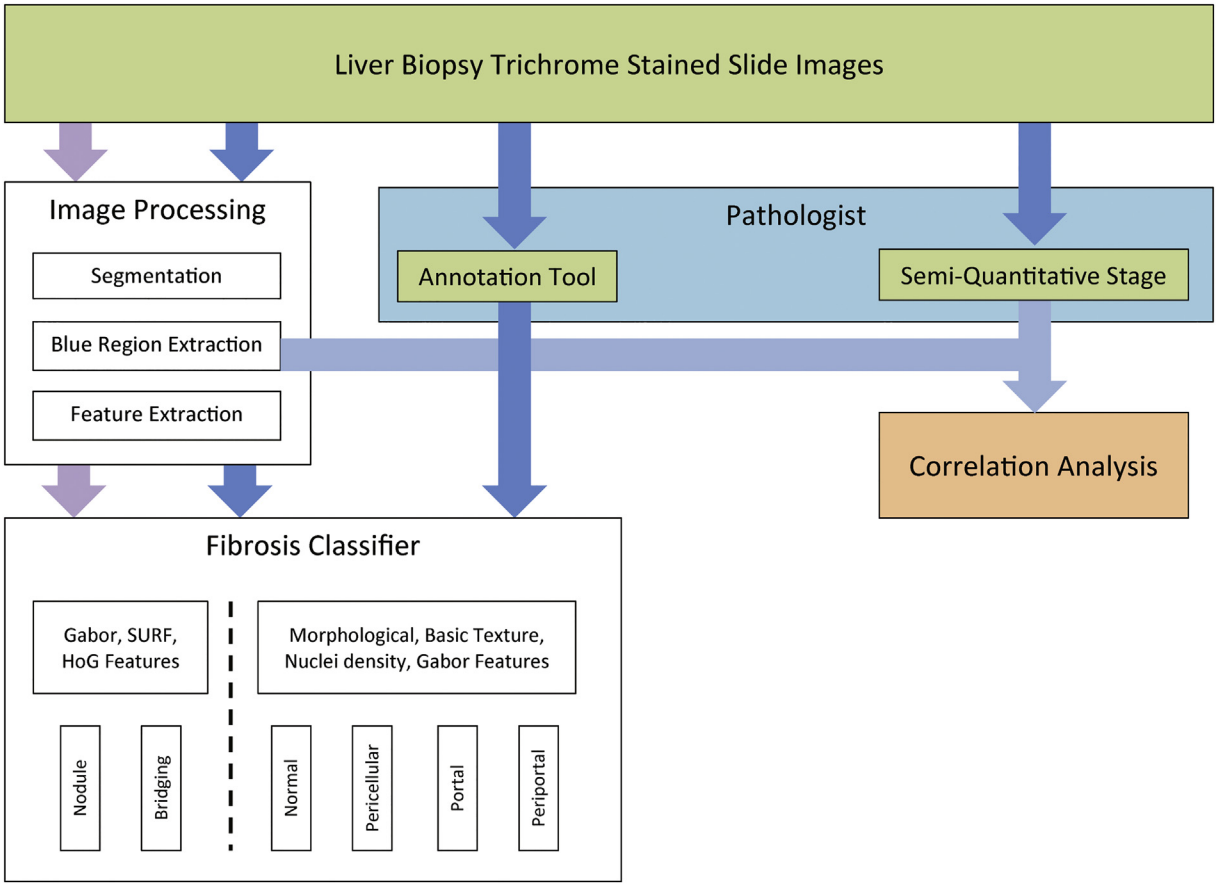

Fig. 3. The flow diagram showing the steps involved in extracting the collagen in a liver biopsy and identifying the different types of fibrosis.

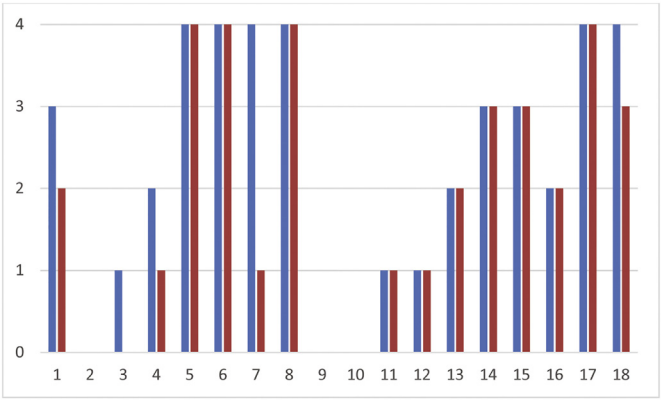

Fig. 4. A bar graph which shows semi-quantitative grades given by both pathologist DEK (blue) and pathologist OWC (red) for the given set of 18 human liver slides. (For interpretation of the references to color in this figure legend, the reader is referred to the web version of this article.)

excellent for detecting normal fibrosis, bridging fibrosis, and presence of nodule/cirrhosis (AUROC > 90% for all). The precision and recall of the classifier for detecting different fibrosis types are shown in Table 1 and the confusion matrix for each fibrosis pattern are provided in the supplementary material labeled confusion matrix.

4. Discussion

Data presented in this study show that accurate automated quantification of hepatic fibrosis and detection of its architectural patterns is possible in NAFLD liver biopsies. This is the first work that presents one integrated AI-automated tool to perform both tasks in NAFLD.

Automated quantification of CPA as a continuous measure of hepatic fibrosis offers several benefits. These include reproducibility and sensitivity to detecting changes in fibrosis that could be missed by manual scoring systems utilizing limited (0–4 or 0–6) semi-quantitative bins [9,11,15,22,23].

Prior studies of CPA in the setting of viral hepatitis demonstrated high correlation of CPA with pathologists' semi-quantitative scores [14,16-21]. Our study and two recent studies show similar correlation of CPA with the liver semi-quantitative fibrosis stages in the setting of NAFLD [35,36].

The demonstrated additional benefits of using CPA in predicting development of clinical outcomes in patients with chronic liver disease (mostly viral hepatitis) [24,28-30] have recently been shown in patients with NAFLD. In a recent European study in 437 patients with biopsy-proven NAFLD [36], CPA independently predicted hepatic decompensation or liver-related death [Hazard Ratio (HR): 1.04 per 1% increase, 95% CI: 1.01–1.08)]. A recent US study analyzed the data from 475 patients with NASH with bridging fibrosis or compensated cirrhosis who enrolled in two phase 2b, randomized controlled trials of simtuzumab [31]. Due to inefficacy, both trials were ended after 96 weeks. Baseline CPA was independently associated with progression of fibrosis to stage 4 (cirrhosis) in those starting with stage 3 fibrosis (HR: 1.44, 95% CI: 1.08–1.91), and in those starting with cirrhosis, CPA was independently associated with increased risk of liver-related clinical events such as ascites, variceal bleeding or encephalopathy (HR: 1.19, 95% CI:1.03–1.38). These data suggest that measurement of CPA in baseline liver biopsies performed as part of clinical care or participation in clinical trials for NAFLD and NASH may provide important prognostic data to identify patients with NAFLD at highest risk for hepatic decompensation or liver related death.

A.

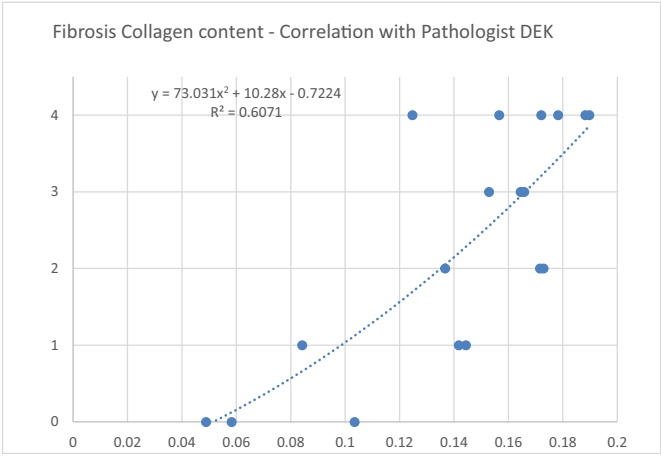

B.

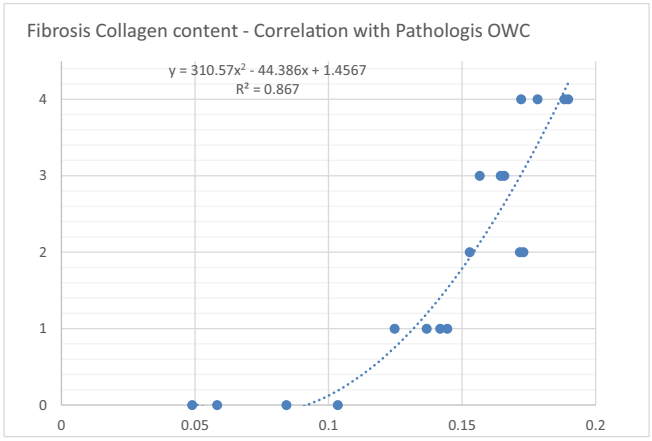

Fig. 5. A) A scatter plot showing correlation between model-computed percentage collagen content for human biopsies with respect to pathologist DEK stage. B) A scatter plot showing correlation between model-computed percentage collagen content for human biopsies with respect to pathologist OWC stage.

Table 1
The precision, recall, and area under the ROC measures for different pattern of fibrosis detection.

Fibrosis pattern	Precision	Recall	AUROC
Normal	85.6	83.3	91.9
Pericellular	76.6	82.7	83.3
Periportal	72.1	76.9	78.6
Portal	77	84.4	86.4
Bridging	84.9	91.7	93
Nodule	89.8	91.6	95.4

However, despite these advantages, CPA does not alone offer a global assessment of hepatic fibrosis. Our study also demonstrates that the relationship between CPA and fibrosis stage is not linear [35], but there is considerable overlap in CPA values across different fibrosis stages. Therefore, the discernment of the architectural distribution or pattern of fibrosis may not be reliably inferred from CPA values. This distinction is important as the clinical management of a patient with NASH and stage 2 (perisinusoidal and portal/periportal) fibrosis is considerably different from that of a patient with NASH and stage 4 fibrosis (cirrhosis) having a similar CPA. The latter patient would usually be under close clinical care and surveyed regularly for development of complication of cirrhosis such as esophageal varices and hepatocellular carcinoma [38]. Thus, we argue that integrating continuous measurement of hepatic fibrosis by CPA with identification of the location and architectural pattern of fibrosis in patients with NAFLD would offer complimentary and global assessment of fibrosis with the clinical and research advantages of both of these assessments.

The CPA classifier correlation was stronger with pathologist OWC's than pathologist DEK's staging of fibrosis. It is important to note that annotations provided by DEK were used for training the fibrosis pattern classifier, not the CPA classifier. The CPA classifier did not use these annotations but rather relied on blue color extraction followed by calculation of the percent of the blue region area to the total tissue area. Even though the two expert liver pathologists are consistent in the use of the same scoring system for staging fibrosis, application of the system's criteria varied slightly between the two pathologists where OWC generally seemed to require higher degree of collagen deposition (CPA) than DEK for stage 4 assignment (Fig. 5).

In one case, there was a 2-stage difference in assessing the severity of fibrosis by the two study pathologists. This case illustrates the challenge of inter-observer variability in assessment of histological features of NAFLD, as we and others had previously reported [12,13,46]. This further highlights the role automated, precise and reproducible methods for assessing fibrosis could play in reducing human variability in detecting and quantifying fibrosis in the setting of NAFLD.

The performance of the automated classifier for detection of different patterns of fibrosis is better on the extremes of fibrosis [stages 0, 3, and 4 (normal fibrosis, bridging, cirrhotic nodules) with AUROC > 90%) compared to intermediate stages [stages 1–2 (pericellular/portal/periportal), AUROC 78–86%], echoing pathologists experience in real practice where recognition of the extremes of fibrosis is usually less challenging and more agreed upon between pathologists. We believe our classifier's performance for detecting the intermediate stages can be refined and improved in future experiments by using additional expert pathologists' annotations for architectural patterns in the intermediate stages of fibrosis.

In summary, we demonstrate that comprehensive automated assessment of hepatic fibrosis in human NAFLD is feasible and accurate. Our automated tool could provide both continuous measurement of amount of fibrosis (CPA) as well as detect the pattern of fibrosis distribution in NAFLD liver biopsies.

Supplementary data to this article can be found online at https://doi.org/10.1016/j.anndiagpath.2020.151518.

Financial support

This research did not receive any specific grant from funding agencies in the public, commercial, or not-for-profit sectors.

Declaration of competing interest

None

References

[1] Tsuchida T, Friedman SL. Mechanisms of hepatic stellate cell activation. Nat Rev Gastroenterol Hepatol 2017;14(7):397–411.
[2] Campana L, Iredale JP. Regression of liver fibrosis. Semin Liver Dis 2017;37(1):1–10.
[3] The French METAVIR Cooperative Study Groupeditor. Intraobserver and interobserver variations in liver biopsy interpretation in patients with chronic hepatitis C. Hepatology 1994;20(1 Pt 1):15–20.
[4] Ishak K, Baptista A, Bianchi L, et al. Histological grading and staging of chronic hepatitis. J Hepatol 1995;22(6):696–9.
[5] Brunt EM, Janney CG, Di Bisceglie AM, Neuschwander-Tetri BA, Bacon BR. Nonalcoholic steatohepatitis: a proposal for grading and staging the histological lesions. Am J Gastroenterol 1999;94(9):2467–74.
[6] Kleiner DE, Brunt EM, Van Natta M, et al. Design and validation of a histological scoring system for nonalcoholic fatty liver disease. Hepatology 2005;41(6):1313–21.
[7] Bedossa P, Carrat F. Liver biopsy: the best, not the gold standard. J Hepatol 2009;50(1):1–3.

[8] Machado MV, Cortez-Pinto H. Non-invasive diagnosis of non-alcoholic fatty liver disease. A critical appraisal. J Hepatol 2013;58(5):1007–19.
[9] Masseroli M, Caballero T, O'Valle F, Del Moral RM, Perez-Milena A, Del Moral RG. Automatic quantification of liver fibrosis: design and validation of a new image analysis method: comparison with semi-quantitative indexes of fibrosis. J Hepatol 2000;32(3):453–64.
[10] O'Brien MJ, Keating NM, Elderiny S, et al. An assessment of digital image analysis to measure fibrosis in liver biopsy specimens of patients with chronic hepatitis C. Am J Clin Pathol 2000;114(5):712–8.
[11] Goodman ZD, Becker Jr. RL, Pockros PJ, Afdhal NH. Progression of fibrosis in advanced chronic hepatitis C: evaluation by morphometric image analysis. Hepatology 2007;45(4):886–94.
[12] Younossi ZM, Gramlich T, Liu YC, et al. Nonalcoholic fatty liver disease: assessment of variability in pathologic interpretations. Mod Pathol Off J U S Can Acad Pathol, Inc 1998;11(6):560–5.
[13] Gawrieh S, Knoedler DM, Saeian K, Wallace JR, Komorowski RA. Effects of interventions on intra- and interobserver agreement on interpretation of nonalcoholic fatty liver disease histology. Ann Diagn Pathol 2011;15(1):19–24.
[14] Huang Y, de Boer WB, Adams LA, et al. Image analysis of liver collagen using sirius red is more accurate and correlates better with serum fibrosis markers than trichrome. Liver Int 2013;33(8):1249–56.
[15] Caballero T, Perez-Milena A, Masseroli M, et al. Liver fibrosis assessment with semiquantitative indexes and image analysis quantification in sustained-responder and non-responder interferon-treated patients with chronic hepatitis C. J Hepatol 2001;34(5):740–7.
[16] Calvaruso V, Burroughs AK, Standish R, et al. Computer-assisted image analysis of liver collagen: relationship to Ishak scoring and hepatic venous pressure gradient. Hepatology 2009;49(4):1236–44.
[17] Lazzarini AL, Levine RA, Ploutz-Snyder RJ, Sanderson SO. Advances in digital quantification technique enhance discrimination between mild and advanced liver fibrosis in chronic hepatitis C. Liver Int 2005;25(6):1142–9.
[18] Zhou Y, Ru GQ, Yan R, et al. An inexpensive digital image analysis technique for liver fibrosis quantification in chronic hepatitis B patients. Ann Hepatol 2017;16(6):881–7.
[19] Campos CF, Paiva DD, Perazzo H, et al. An inexpensive and worldwide available digital image analysis technique for histological fibrosis quantification in chronic hepatitis C. J Viral Hepat 2014;21(3):216–22.
[20] Stasi C, Tsochatzis EA, Hall A, et al. Comparison and correlation of fibrosis stage assessment by collagen proportionate area (CPA) and the ELF panel in patients with chronic liver disease. Dig Liver Dis 2019;51(7):1001–7.
[21] Yegin EG, Yegin K, Karatay E, et al. Quantitative assessment of liver fibrosis by digital image analysis: relationship to Ishak staging and elasticity by shear-wave elastography. J Dig Dis 2015;16(4):217–27.
[22] Matalka II, Al-Jarrah OM, Manasrah TM. Quantitative assessment of liver fibrosis: a novel automated image analysis method. Liver Int 2006;26(9):1054–64.
[23] Pavlides M, Birks J, Fryer E, et al. Interobserver variability in histologic evaluation of liver fibrosis using categorical and quantitative scores. Am J Clin Pathol 2017;147(4):364–9.
[24] Nielsen K, Clemmesen JO, Vassiliadis E, Vainer B. Liver collagen in cirrhosis correlates with portal hypertension and liver dysfunction. APMIS: Acta Pathol Microbiol Immunol Scand 2014;122(12):1213–22.
[25] Isgro G, Calvaruso V, Andreana L, et al. The relationship between transient elastography and histological collagen proportionate area for assessing fibrosis in chronic viral hepatitis. J Gastroenterol 2013;48(8):921–9.
[26] Murakami Y, Abe T, Hashiguchi A, Yamaguchi M, Saito A, Sakamoto M. Color correction for automatic fibrosis quantification in liver biopsy specimens. J Pathol Inform 2013;4:36.
[27] Sethasine S, Jain D, Groszmann RJ, Garcia-Tsao G. Quantitative histological-hemodynamic correlations in cirrhosis. Hepatology 2012;55(4):1146–53.
[28] Manousou P, Dhillon AP, Isgro G, et al. Digital image analysis of liver collagen predicts clinical outcome of recurrent hepatitis C virus 1 year after liver transplantation. Liver Transpl 2011;17(2):178–88.
[29] Huang Y, de Boer WB, Adams LA, MacQuillan G, Bulsara MK, Jeffrey GP. Image analysis of liver biopsy samples measures fibrosis and predicts clinical outcome. J Hepatol 2014;61(1):22–7.
[30] Tsochatzis E, Bruno S, Isgro G, et al. Collagen proportionate area is superior to other histological methods for sub-classifying cirrhosis and determining prognosis. J Hepatol 2014;60(5):948–54.
[31] Sanyal AJ, Harrison SA, Ratziu V, et al. The natural history of advanced fibrosis due to nonalcoholic steatohepatitis: data from the Simtuzumab trials. Hepatology 2019;70(6):1913–27.
[32] Fontana RJ, Goodman ZD, Dienstag JL, et al. Relationship of serum fibrosis markers with liver fibrosis stage and collagen content in patients with advanced chronic hepatitis C. Hepatology 2008;47(3):789–98.
[33] Hall AR, Tsochatzis E, Morris R, Burroughs AK, Dhillon AP. Sample size requirement for digital image analysis of collagen proportionate area in cirrhotic livers. Histopathology 2013;62(3):421–30.
[34] Stasi C, Leoncini L, Biagini MR, et al. Assessment of liver fibrosis in primary biliary cholangitis: comparison between indirect serum markers and fibrosis morphometry. Dig Liver Dis 2016;48(3):298–301.
[35] Masugi Y, Abe T, Tsujikawa H, et al. Quantitative assessment of liver fibrosis reveals a nonlinear association with fibrosis stage in nonalcoholic fatty liver disease. Hepatol Commun 2018;2(1):58–68.
[36] Buzzetti E, Hall A, Ekstedt M, et al. Collagen proportionate area is an independent predictor of long-term outcome in patients with non-alcoholic fatty liver disease. Aliment Pharmacol Ther 2019;49(9):1214–22.
[37] Younossi ZM, Koenig AB, Abdelatif D, Fazel Y, Henry L, Wymer M. Global epidemiology of nonalcoholic fatty liver disease-meta-analytic assessment of prevalence, incidence, and outcomes. Hepatology 2016;64(1):73–84.
[38] Chalasani N, Younossi Z, Lavine JE, et al. The diagnosis and management of nonalcoholic fatty liver disease: practice guidance from the American Association for the Study of Liver Diseases. Hepatology 2018;67(1):328–57.
[39] Angulo P, Kleiner DE, Dam-Larsen S, et al. Liver fibrosis, but no other histologic features, is associated with long-term outcomes of patients with nonalcoholic fatty liver disease. Gastroenterology 2015;149(2):389–397 e310.
[40] Vilar-Gomez E, Calzadilla-Bertot L, Wai-Sun Wong V, et al. Fibrosis severity as a determinant of cause-specific mortality in patients with advanced nonalcoholic fatty liver disease. Gastroenterology 2018;155(2):443–57.
[41] Kleiner DE. Histopathology, grading and staging of nonalcoholic fatty liver disease. Minerva Gastroenterol Dietol 2018;64(1):28–38.
[42] Gawrieh S, Chalasani N. Emerging treatments for nonalcoholic fatty liver disease and nonalcoholic steatohepatitis. Clin Liver Dis 2018;22(1):189–99.
[43] Kleiner DE, Bedossa P. Liver histology and clinical trials for nonalcoholic steatohepatitis-perspectives from 2 pathologists. Gastroenterology 2015;149(6):1305–8.
[44] Vanderbeck S, Bockhorst J, Komorowski R, Kleiner DE, Gawrieh S. Automatic classification of white regions in liver biopsies by supervised machine learning. Hum Pathol 2014;45(4):785–92.
[45] Vanderbeck S, Bockhorst J, Kleiner D, Komorowski R, Chalasani N, Gawrieh S. Automatic quantification of lobular inflammation and hepatocyte ballooning in nonalcoholic fatty liver disease liver biopsies. Hum Pathol 2015;46(5):767–75.
[46] Fukusato T, Fukushima J, Shiga J, et al. Interobserver variation in the histopathological assessment of nonalcoholic steatohepatitis. Hepatol Res 2005;33(2):122–7.